Available online at www.garmian.edu.krd

Passer Journal

Passer 6 (Issue 1) (2024) 08-15

http://passer.garmian.edu.krd/

Flexible Wearable Antenna Incorporating Metasurface for Wban Applications

Shene Hamid Ali[1*], Yadgar Ibrahim Abdulkarim[1], Hastyar Omer Mohammed[1]

[1]*Department of Physics, College of Science, University of Charmo, Chamchamal, Kurdistan Region, Iraq.*

Received 13 August 2023; revised 24 October 2023;
accepted 25 October 2023; available online 20 November 2023

DOI: 10.24271/PSR.2023.411415.1369

ABSTRACT

The wireless body area networks (WBAN) have received much interest from researchers in the field of medical application in recent years such as heart rate, temperature monitoring and blood pressure. In this study, a new antenna design with a low profile or easy fabricates introduced (WBAN) applications. In this work, a metasurface technique was used to improve the antenna characteristics, including return loss, gain and radiation patterns. The designed structure, and numerical analysis have been performed by using Computer Simulations Technologies (CST) microwave studio. The structure of the antenna a composite of three layers from top to bottom as follows: radiation copper patch, felt substrate and ground copper. The key idea for this work is loading the MTS structure of a 5 × 5 unit cell to the designed antenna to enhance the antenna parameters. The overall structure thickness is 4.68 mm and the antenna operates between 6 and 14 GHz. According to the results, for the simulation and measurement, the gain increased from 7.33 dBi to 7.47 dBi and from 10.23 dBi to 11.1 dBi with and without MTS, respectively. The antenna was investigated in free space and on a human body both numerically, and experimentally. In addition, the bending evaluation was investigated. The novelties of this work are high gain, wide-band, directional radiation pattern, small size, low profile, and easy fabrication. The experimental, and simulation results are in good agreement. We believe this work can be helpful in future medical applications.

Keywords: Wearable Antennas, Metasurface, (WBAN), and Gain.

1. Introduction

Wearable antennas have achieved significant progress over the past decade and are currently utilized extensively in many kinds of networking contexts, such as sports, combat, rescue, and personal medical monitoring[1-3]. Researchers from industry and academic institutions have recently become interested in wearable textile antennas due to the variety of uses they can have as a component of wireless body area networks (WBAN) systems, including sports, security, medicine, and the military[4]. Due to their low dielectric permittivity, flexible materials are suitable substrates for wearable antenna designs and expand the antenna impedance bandwidth[5, 6]. Among many textiles available, felt[7-10] and denim[6, 11-13] are popular alternatives. The substrate's backside is where a portion of the ground plane is applied, consequently expanding an impedance bandwidth. To expand the bandwidth issue recommended antennas, a portion of the ground beneath the plane was incorporated into this design, towards the backside of the substrate, which likewise uses felt as the substrate material.

* Corresponding author
E-mail address: shene.hamid@charmouniversity.org (Instructor).
Peer-reviewed under the responsibility of the University of Garmian.

Wearable antennas are integrated into within-body, on-body, or off-body devices in a suitable method, making them an essential important component of WBAN systems[14]. A growing number of human accessories, like bright finger rings[15, 16], eyeglasses[17], and intelligent wrist watches, are being created that incorporate wearable antennas[18-22] wireless body area networks (WBAN) communications. Wearable textile antennae provide several critical benefits, such as being lightweight, offering high flexibility, being inexpensive to produce, and being simple to integrate into clothing[23]. The advantages of flexible textiles antenna patches for wearable systems are their low profile, small size, high flexibility, simple fabrication, and simplicity of integration into the garment. For ease of the user, these qualities offer the wearable systems' fundamental criteria, such as flexibility and compactness[24, 25]. Because of their extremely low dielectric constant, textile materials used as antenna substrates aid in lowering surface wave losses and boosting antenna bandwidth[26]. For WBAN applications, several flexible, textile wearable antenna designs, including the monopole[7, 8], inverted-F shaped[9,10], substrate-integrated waveguide[27], and reconfigurable antennas[28], have recently been described.

Numerous numbers of works have been conducted in this area[29]. Recently, simulation and fabrication of a broadband (5.15–5.825 GHz) circularly polarized antenna using felt as a substrate; the

peak of the antenna gain showed achievement at 8.5 dBi and a front-to-back ratio of 25 dB[30]. Design of an antenna for medical body area network applications with a bandwidth of 2.3-2.5 GHz. The results showed front-to-back ratio enhancement by 13 dB compared to the primary antenna and a gain of 6.55 dBi using jeans (denim) as substrate[31]. Bendable 68×38×1.57 mm^3 antenna has been proposed operating between 2.40- 2.52 GHz; the results showed a gain of 6.88 dBi[32]. Also a dual-band design on an artificial magnetic conductor for WBAN applicationshas recently been introduced. The substrate material of the design is felt; the antenna operates in the range of 1-7 GHz and has gain of 9.9 dBi.

In this study, a wearable, flexible UWB antenna for WBAN applications is introduced to address the aforementioned issues above. Itis situated on the part of the ground that is combined of felt substrates and coupled to the MTS component at the back of the structure and copper conductors fabrics material, The showed antenna with the MTS structure has 4.68 millimeters its thickness, which is the lowest thickness for a UWB band antenna with an MTS that has been documented in the literature to date Evaluations of results and compared three-dimensional (3D) electromagnetism (EM) simulations in free space with and without the MTS in its rear of the antenna were used to evaluate The preliminary findings intended low-profile antennas. The findings demonstrated that placing the created MTS The antenna's construction at the back significantly enhances its abilities in terms of gain and radiation pattern while preventing interference between the antenna's fields and the body. Measurements were also taken, and the proposed antenna and MTS structure were successfully produced.

At the end, developed new designs and techniques were used to enhance the performance of wearable antennae for biomedical applications. Finding and proposing a new technique to improve bandwidth and gain of the wearable antenna. Design broadband-high gain antenna with a smaller thickness in comparison to the proposed antennas by worldwide researchers. New design high gain obtained around 11.1 dBi, wideband in the frequency range 6-14 GHz, directional radiation pattern, small size, low profile, and easy fabrication.

The results of measurements and simulations are in good agreement. It has been demonstrated that the suggested MTS-structured antenna, which is is attractive to be applied for WBAN applications.

2. Designs of Antenna and Metasurface Structures

2.1 The design of Antenna

Computer Simulation Technology Studio was utilized to design the antenna this project's antenna, and proposed antenna measures 100 millimeters in width, 70 millimeters in length, and 1 millimeter in height overall. It has a loss tangent of 0.04 and a relative permittivity of 1.4. copper-based metallic layers that make up the radiator patches and ground plane have a conductivity of $1.18x10^5$ S/m and a thickness of 0.17 millimeters. front, back, and one-patch antennas are used in Fig. 1 (a), along with the construction and geometrical characteristics of the developed wearable microstrip antenna. The image represents the substrate as blue and the metallic layers as yellow. Yellow is also used to represent the connector in direct touch with the feed line. The antenna, which is known, comprises a rectangle of radiated patches with the Microstrip feeding to the felt substrates upfront. Suggested that the antenna's rectangle radiator patch design has been extensively and studied. The antenna's bandwidth is increased by circular parasitic patches or rectangle ground plane of the substrate's reverse. Substrate's length and width are as Ls and Ws, respectively. Depicted in Fig. 1(a). The symbols Lp and Wp denote the antenna's length and width, respectively. Additionally, Wf and Lf stand for the feed line's width and length, respectively. However, the ground plane's rectangular shape's width and length are represented by the letters Wg and Lg on the antenna's back, respectively. To account for the radius of the parasitic patch, add an extra r. An electromagnetic modeling tool was used to optimize each geometrical aspect antenna depicted in Fig. 1(a).

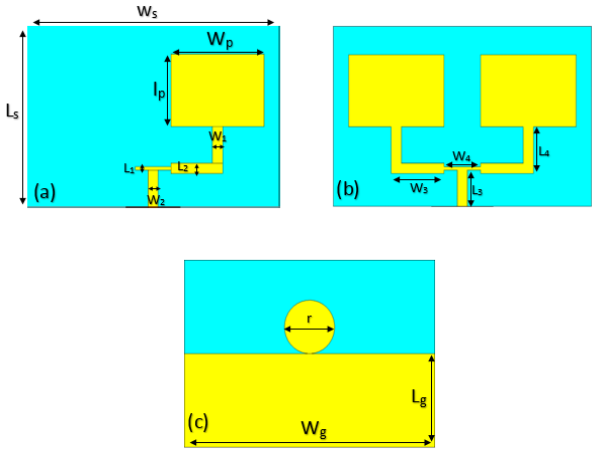

Figure 1: The geometry of a Flexible patch antenna. In blue is the substrate, and in yellow is copper. (a) Front view of one rectangular patch antenna with dimensions lp and Wp, (b) front view of two-patch array antenna, (c) back view of the antenna showing the rectangular plane of copper with dimensions Lg, Wg, and a circle of radius r.

2.2 Metasurface structure design

whenever antenna optimization is done, we create an MTS structure and place it on the antenna's back to lessen interference from a person's body. The S11 parameter, also known as the reflection coefficient, covers the whole working frequency spectrum, and is the primary element to be included within the process that will be used to construct the MTS structure. Felt material with a thickness of 1 millimeter is used as a gap separating the MTS or antennas to establish distance or prevent electrical contact between them. Suggested metasurface structure, which is made up of 25 square and rhombus-shaped unit cells arranged in a 5x5 square lattice, is shown in detail in Figure 2(a). Due to its ease of production, the shape lattice was chosen for the metasurface. Each MTS structure's width (Ws) and length (Ls) are equal to 100 mm in the figure since each metasurface cell's side length is 10 mm. Figure 2(b) displays the antenna's cross-section with the MTS. The MTS structure consists of three different layers as seen in the section view: a dielectric substrate in between 2 metallic (metasurface & ground plane) surfaces. The MTS construction uses felt fabric as the dielectric substrate and copper for the metallic layers much like the antenna design. In contrast to the felt used for the antenna and

the feeling spacer, the felt fabric utilized in the MTS construction is 2 millimeters thick.

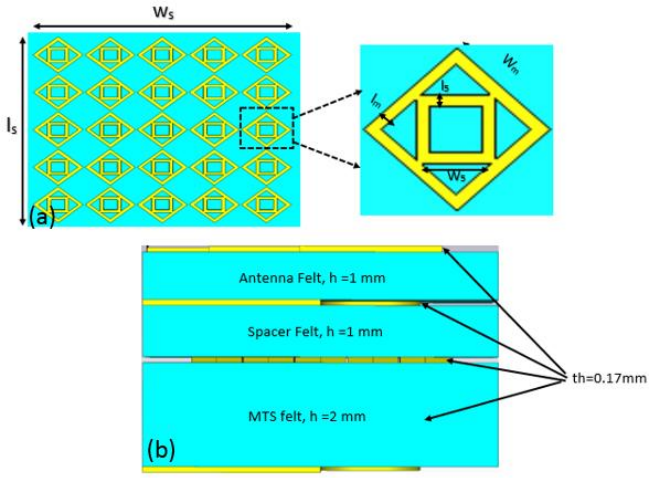

Figure 2: The antenna design with 5x5 array meta surface unit cells (blue: felt, yellow: copper). (a) MTS structure front view showing 25 square and rhombus shape of the cells of the MTS (b) Side view of the final proposed structure which is a combined antenna and MTS.

Table 1: lists all of the prototype's parameters that have been optimized.

parameter	Value (mm)	Parameter	Value (mm)	parameter	Value (mm)
Ws	100	Wm	5	W3	20.5
Ls	70	Lm	1	L3	14.12
Wg	100	W1	4	W4	14.12
Lg	35	L1	1.31	L4	18.12
Wp	37	W2	4	W5	3
Lp	24	L2	4	L5	1
r	10				

Furthermore, designed antenna elements are fabricated as given in Figure 3. The single antenna component is shown in Figure 3(a), and an array of antennae with back side resonators are given also in Figure 3(b) and c, respectively. In the fabrication processes, a felt material and copper tape are used to implement the proposed antenna. Moreover, an SMA port is connected to the feeding line as illustrated. This fabrication technique is a manual technique that has disadvantages and can cause some losses in the antenna performance.

Figure 3: Fabricated prototype of the proposed antenna, where antenna structure consists of the patch(copper), substrate (felt), and ground (copper), (a) front view of one patch antenna, (b) front view of array antenna, and (c) back side view antenna.

In another fabrication process, the designed metasurface has been fabricated in the lab, as explained in the previous paragraph. Figure 4(a) shows the fabricated metasurface layer in 5x5 periodic arrangements. Figure 4(b) or c illustrates S11 measurement setups of the single and array antenna configurations. In measurements, an Agilent PNA-L vector network analyzer has been used, as shown in the figure. Before the measurement of antenna elements, calibration processes have been done step by step, and their measures have been created.

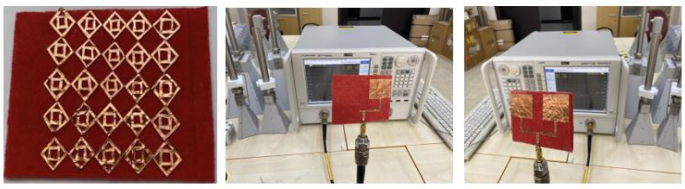

Figure 4: Fabricated prototype of the proposed antenna, (a) MTS structure Front view, (b) Experimental view of one patch antenna, (c) fabricated two patch antenna measured view.

3. Results of Simulation and Measurement

3.1 Gain and reflection coefficient

In this part, patch antennas, antennas with and without MTS, have been compared in terms of acquired gain and reflection coefficient. while the simulations were completed, S11 was evaluated in a laboratory setup. during simulations, S11 was put to the test in the lab. The calculated and measured frequency-dependent change of the S_{11} value in the frequency range is shown in Figure 5(a). Despite some frequencies having a little change reflection coefficient and shifting resonance frequencies, according to measurement results given in Fig. 6(a), The estimated and actual simulations and test results provided in Fig 5. are compatible with the antenna's broad frequency level, which runs from 6 gigahertz toward 14 gigahertz. Then, with the MTS construct installed before the antennas, measuring the S11 reflection coefficient parameter for the one patch antenna for the antenna with and without MTS was carried out. Since S11 is less than or about - 10 dB, this antenna can operate between 6 GHz and 14 Gigahertz. Antenna's simulated gain vs. frequency graph is provided to compare an antenna with and without MTS. Fig5(b) contrasts simulated gain for a patch antenna, an antenna without MTS, and with MTS. in the simulation antenna without MTS, the highest gain was 7.33 db at 10.032 GHZ, and in the antenna with MTS, the highest gain at 7.47 db at 9.8 GHZ. Fig(6) displays the measured realized gain between antennas without and with MTS. Across the whole operating frequency range, it is clear an antenna with MTS has more significant gain than antennas without MTS.

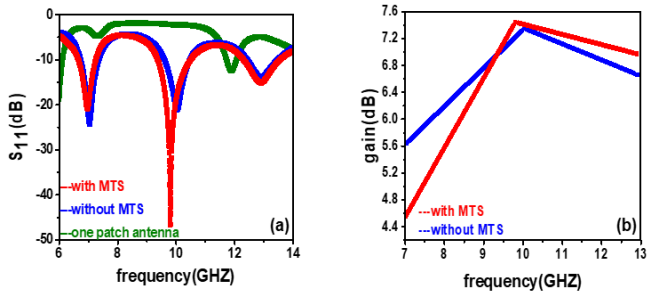

Figure 5: Effect of MTs on antenna reflection coefficient and gain. (a) Simulated result for reflection coefficient without MTS, with MTS, and one patch antenna, (b)The simulated gain without MTS, with MTS, for the proposed structure.

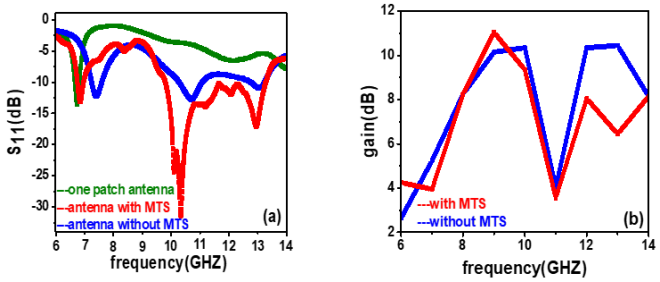

Figure 6: Results of reflection coefficient and gain for the fabricated antenna (a) measurement result for reflection coefficient without MTS and with MTS, and one patch (b)The measurement gain without MTS and with MTS.

3.2 Radiation pattern

The projected 2D radiating patterns from the antenna without and with the MTS, located in the xz (phi 0) or yz (phi 90) directions design, are shown in figures 7, 8, and 9 correspondingly. The antenna with the MTS structure demonstrated more significant directed radiation than antennas devoid of MTS construction. Planned MTS improves strength along the bore's side. Surface waves are lowered by the structure. This demonstrates how better radiation properties like gain, directionality, reflection coefficient (S_{11}), are made possible by the usage of the MTS. Additionally, in a polar coordinate system, The designed antenna's far-field radiating patterns, both with and without MTS construction, are displayed within an empty area. These patterns were computed by simulations to frequency ranges of about 7.04 gigahertz or 10.032 gigahertz and 12.904 gigahertz , respectively. As a result, the human body is exposed to and absorbs lower electromagnetic radiation. Figures 10, 11, 12, and 13 display the measured 2D radiation patterns at resonance frequencies in major sectors.

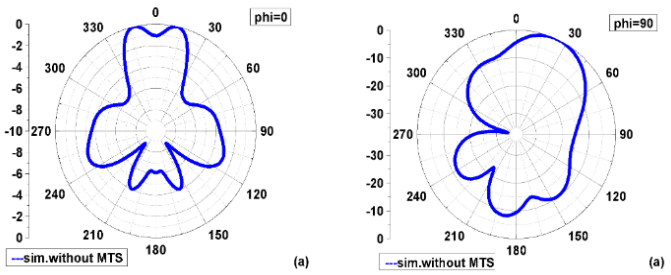

Figure 7: Simulated 2D radiation pattern of the proposed antenna without MTS (a) at 7.04 GHZ Phi= 0 , (b) at 7.04 GHZ Phi= 90.

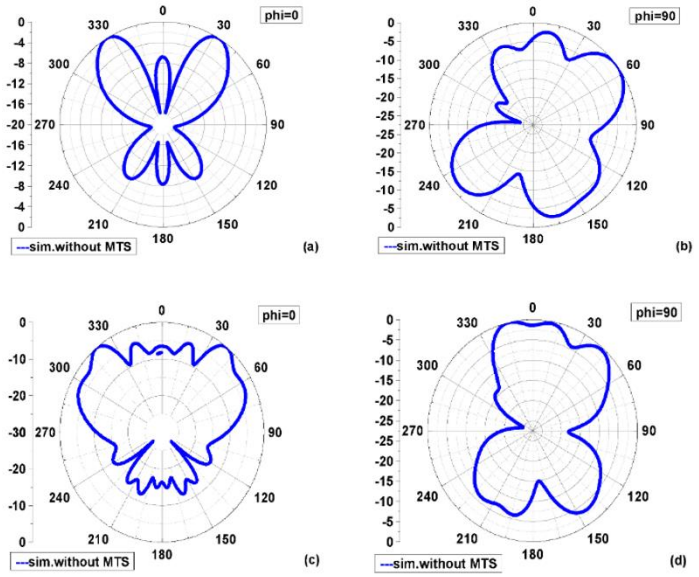

Figure 8: Simulated 2D radiation pattern of the proposed antenna without MTS (a) at 10.032 GHZ phi=0, (b) at 10.032 GHZ phi=90, (c) at 12.904 GHZ Phi= 0 ,(d) at 12.904 GHZ Phi= 90.

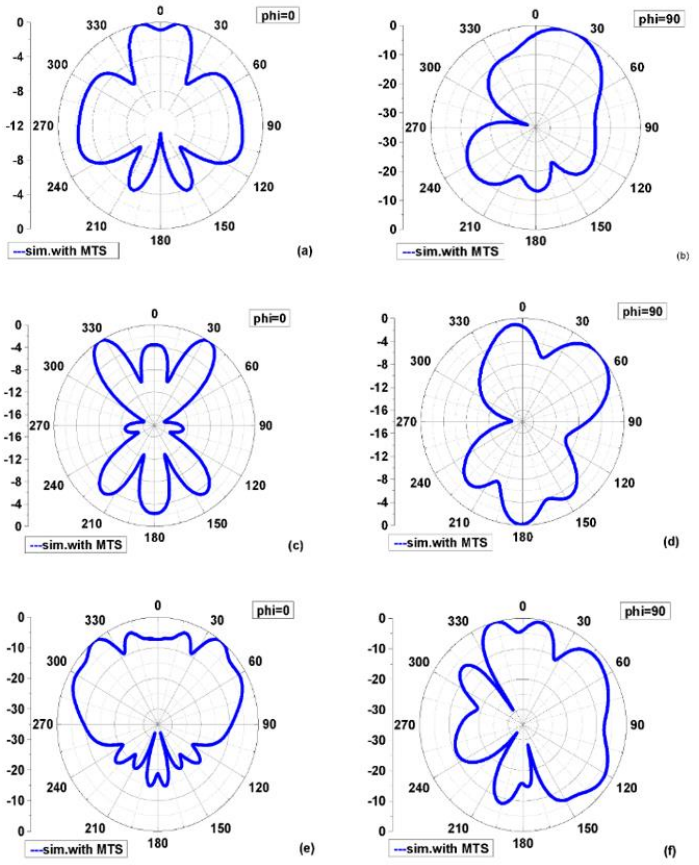

Figure 9: Simulated 2D radiation pattern of the proposed antenna with MTS (a) at 6.968 GHZ Phi= 0, (b) at 6.968 GHZ Phi= 90, (c) at 9.8 GHZ Phi= 0, (d) at 9.8 GHZ Phi= 90, (e) at 12.888 GHZ phi=0, (f) at 12.888 GHZ phi=90.

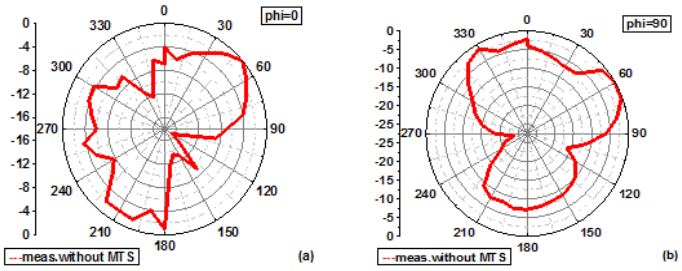

Figure 10: measured 2D radiation pattern of the proposed antenna without MTS (a) at 7 GHZ Phi= 0 , (b) at 7 GHZ Phi=90 .

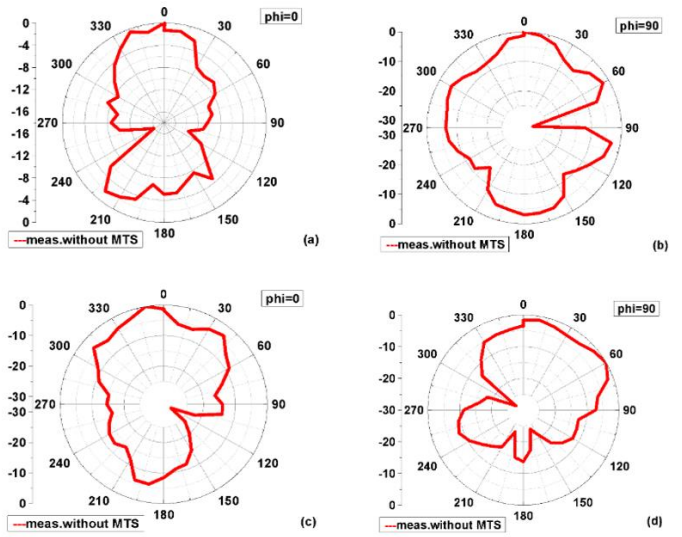

Figure 11: measured 2D radiation pattern of the proposed antenna without MTS(a) at 10 GHZ phi=0, (b) at 10 GHZ phi=90. (c) at 12.9 GHZ Phi= 0, (d) at 12.9 GHZ Phi=90.

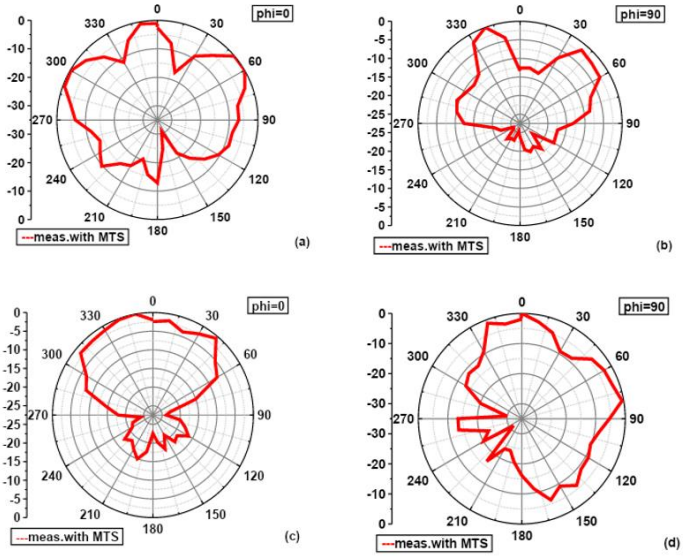

Figure 12: measured 2D radiation pattern of the proposed antenna with MTS (a) at 7 GHZ Phi= 0, (b) at 7 GHZ Phi=90 , (c) at 10 GHZ Phi= 0 , (d) at 10 GHZ Phi= 90 .

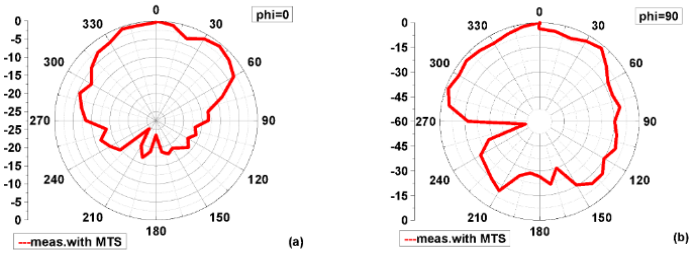

Figure 13: measured 2D radiation pattern of the proposed antenna with MTS(a) at 12.9 GHZ phi=0, (b) at 12.9 GHZ phi=90.

4. On Body Antenna Performance

The human body absorbs some electromagnetic energy and reflects part of it when a wearable antenna is placed on it. Determining how the proposed antenna will function over time and what effect it will have on the body of a person is therefore vitally important. The simulation program, the human body is modeled a rectangular body, and in the simulations we performed, we employed this model. The body model is shown in Fig. 14. 4 levels of the human body's tissues compose the human organism's model, from outside to inside, as depicted in the image: skin, fat, muscle, and bone. In the modeled geometry, which has overall diameters of 100 millimeters, 100 millimeters, and 23 millimeters, skins, fat, muscles, or bones layers, respectively, one point seven millimeters, eight millimeters, ten millimeters, and three-point three millimeters thickness. Body's layer thicknesses are similar to those documented in the literature. Additionally, The CST program's material library contains definitions that establish the material's density or dielectric constant quantities of physiological organs utilized in simulations. Table 2 shows the permanent density of material or dielectric factors used simulated at different frequencies.

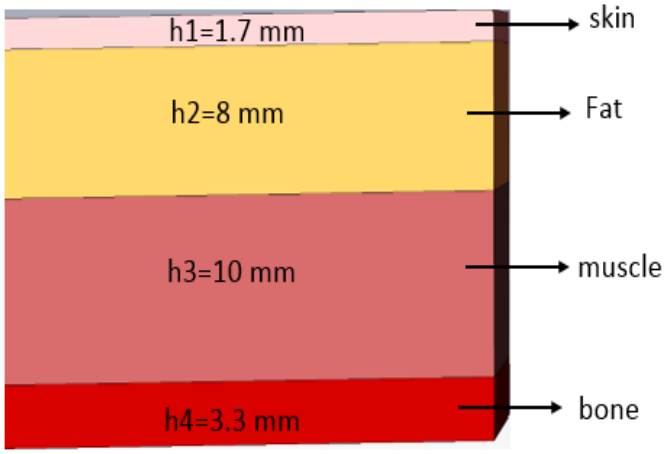

Figure 14: Cubic body tissue model showing the four different tissue layers from top to bottom: skin, fat, muscle, and bone with their corresponding thicknesses.

Table 2: lists the material density and electrical properties of the simulated human body tissues.

				7.04 GHZ		10.032 GHZ	
Tissue type	**Density (Kg/m^3) [33]**	**Specific heat Capacity (KJ/K×kg) [33]**	**Thermal conductivity (W/K×m) [33]**	**Electric or Effective Conductivity (S/m) [33]**	**Effective dielectric permittivity (F/m) [33]**	**Electric or Effective Conductivity (S/m) [34]**	**Effective dielectric permittivity (F/m) [34]**
skin	11.09	3.39	0.37	34.06	4.85	8.0138	31.29
fat	119	2.34	0.21	4.85	1.06	0.58521	4.6023
muscle	1190	3.42	0.49	47.8	6.5	10.626	42.764
bone	1850	1.31	0.40	9.1	1.45	1.98	8.31

As shown, In both actual and hypothetical places, the bodily tissue's dielectric constant values change often. To the planned antenna and MTS were applied the body of a human model before the simulations were run. Simulations with the body model and the anticipated antenna were rerun without it to examine the effects of the suggested MTS structure. In all cases—MTS structure present or absent— The antenna's separation from the body model was maintained at 3.34 millimeters. Measurements were also made using the produced antenna prototype and the MM structure prototype. While performing our investigation, we used the MTS and the allocated antenna. The average distance within the antenna or our bodies during the experiments was three point thirty-four millimeters, and in the simulations, the distance was the same (See Fig. 2(b), when the total thickness for spacers felt, metasurface, MM felt, or MM ground is 3.34 millimeter). In simulations, as was employed. Figure 15(a) shows the differences for a patch antenna between the graphs for the empty space and on-body scenarios., whereas Figure 15(b) shows the changes for the graphs of the free space and on-body cases. Of an antenna without MTS are displayed. Changes in S11 characteristics are illustrated for a body model one patch antenna, the intended antenna in open space, and for antenna without or with the MTS structure. With frequency estimated in simulations. On the other hand, in Fig. 15, the graphs of the on-body and free space instances of an antenna with MTS are different (c).

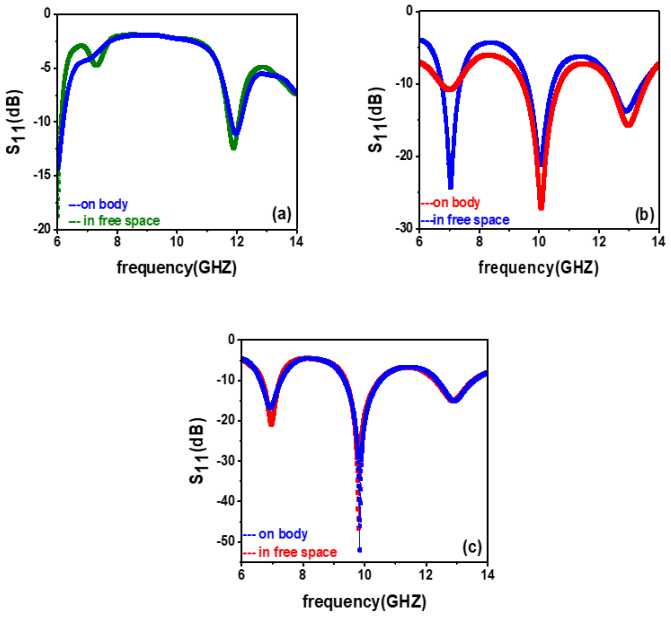

Figure 15: Simulated reflection coefficient (S11) showing on the body and free space performance (a) one-patch antenna, (b) reflection coefficient S11 of the proposed two-patch antenna without MTS, and (c) S11 for the proposed antenna with MTS.

5. Bending Evaluation

The adaptability and user comfort of wearable antennae are heavily regarded for real-world requirements. The behavior of wearable antennae should be investigated in terms of robustness and durability under various deformations. The wearable antenna is expected to be distorted for different applications, incorporating body area networks exclusively. This is especially true when it is loaded upon the human being. The performance of the MTM-incorporated antenna in free space must, therefore, be evaluated. The effects of body loading will then be studied to ensure its uniformity. As shown in Figure 16, In the CST MWS, the Different antenna curvatures result from these diameter variances. They chose using the dimensions of models of adult people's legs and arms. To validate the simulation's findings, measurements were conducted using Styrofoam cylinders of appropriate sizes. Recommended design is bent onto vacuum cylinders that have diameters of 50, 60, 70, and 80 mm. The proposed designs of S_{11} with various bending diameters are shown in Figure 17A–D. As can be observed, for all diameter values along the y-axis, Still under ten dB separates the target frequency of 7.03 Gigahertz.

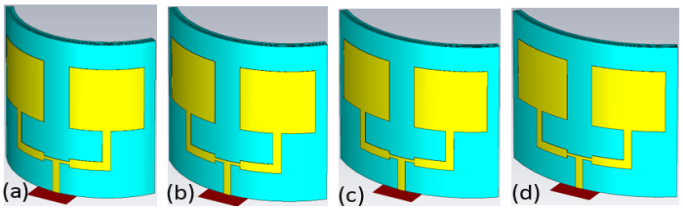

Figure 16: Simulated antenna combined with MTS bent with different radii. (a) diameter d=50mm (b) d= 60mm (c) d=70mm, and (d) d= 80 mm.

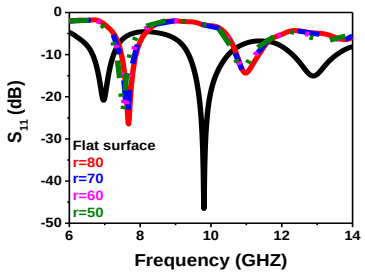

Figure 17: Measured S11 plots of the proposed antenna combined with MTS in different bending conditions in free space.

Conclusion

In summary, we proposed and investigated a new antenna with a low cost, small in size, stable, easy to fabricate, has high sensitivity, and thickness of 4.68 mm to be operated in the ultra-wideband frequency range from 6 to 14 GHz both numerically and experimentally. Computer Simulation Technology (CST) Microwave Studio 2018 was used to obtain the simulation results. The key idea for this work is loading the MTS structure of a 5 × 5 unit cell to the designed antenna to enhance the antenna parameters. According to the data, for the simulation and measurable results, the gain increased from 7.33 dBi to 7.47 dBi and from 10.23 dBi to 11.1 dBi with and without MTS, respectively. To the best of our knowledge, it is the lowest thickness reported in the literature for UWB antennas with MTS. The proposed is designed and manufactured using fully flexible textiles. This design of wearable antennas with MTS topology for WBAN applications was designed numerically and experimentally. Both the MTS structure and the suggested antenna were built with entirely flexible materials. The proposed antenna's measured and simulated results were compared with and without the MTS construction. Respectively. Antenna's radiating pattern was more uniform when it had an MTS construction, which is essential in WBAN applications. In addition, The designed antenna was simulated in free space and on the human body model without MTS and with MTS structure, and bending evolution with different radii (50-, 60-, 70-, and 80-mm) has been presented. The antenna can be suitable candidate for use in medicine and WBAN applications. Measurement results are in good agreement with the results found in the simulations. It shows that the proposed antenna is very a suitable for WBAN applications due to its low thickness, high gain, and low cost.

Authors contribution

Conceptualization: Sh.H.A. and Y.I.A., methodology: Sh.H.A. and Y.I.A., software: Sh.H.A., investigation: Sh.H.A., Y.I.A. and H.O.M., writing—original draft preparation: Sh.H.A., H.O.M. and Y.I.A., supervision, Y.I.A. and H.O.M., writing—review and editing: Y.I.A. and H.O.M., figures and tables: Sh.H.A.. The manuscript's published form was approved by all authors after they had read it.

Acknowledgements

We thank Professor Muharrem Karaaslan and Dr. Fatih Özkan Alkurt at Department of Electrical-Electronics Engineering, Iskenderun Technical University, Hatay, Turkey, for their fabrication of our prototype and recommendations. The authors highly appreciate Charmo University's Department of Physics permission to use a workstation computer to run the numerical simulations. This research work has not received funds, but the expenses covered by the authors themselves.

References

1. k. N. Paracha *et al.*, "a low profile, dual-band, Dual-polarized antenna for indoor/outdoor wearable application," *IEEE Access*, vol. 7, pp. 33277–33288, 2019, DOI: 10.1109/access.2019.2894330.
2. S. Yan, V. Volskiy, and G. A. E. Vandenbosch, "Compact dual-band textile PIFA for 433-mhz/2.4-ghz ism bands," *IEEE antennas WIREL. Propag. Lett.*, vol. 16, pp. 2436–2439, 2017.
3. J. Kim, A. S. Campbell, B. E.-F. De ávila, and J. Wang, "wearable biosensors for healthcare monitoring.," *nat. BIOTECHNOL.*, vol. 37, no. 4, pp. 389–406, APR. 2019, DOI: 10.1038/s41587-019-0045-y.
4. H. M. S. Shakhirul, M. Jusoh, A. Sahadah, C. M. Nor and A. Rahim, "Embroidered wearable textile antenna on bending and wet performances for UWB reception," *MICROW. Opt.*, vol. 48, no. 12, pp. 2611–2615, 2014, DOI: 10.1002/mop.
5. R. Salvado, C. Loss, gon, and P. Pinho, "Textile materials for the design of wearable antennas: a survey," *sensors (SWITZERLAND)*, vol. 12, no. 11, pp. 15841–15857, 2012, DOI: 10.3390/s121115841.
6. A. Mersani, l. Osman, and J.-M. Ribero, "Design of a textile antenna with artificial magnetic conductor for wearable applications," *MICROW. Opt. Technol. Lett.*, vol. 60, pp. 1343–1349, Jun. 2018, DOI: 10.1002/mop.31158.
7. S. Yan, l. A. Y. Poffelie, P. J. Soh, X. Zheng, and G. A. E. Vandenbosch, "On-body performance of wearable UWB textile antenna with full ground plane," in *2016 10th EUROPEAN conference on antennas and propagation (EUCAP)*, 2016, pp. 1–4. Doi: 10.1109/eucap.2016.7481477.
8. S. Mohandoss, S. K. Palaniswamy, R. R. Thipparaju, m. Kanagasabai, b. R. Bobbili naga, and s. Kumar, "On the bending and time domain analysis of compact wideband flexible monopole antennas," *AEU - int. J. Electron. Commun.*, vol. 101, pp. 168–181, 2019, DOI: https://doi.org/10.1016/j.aeue.2019.01.015.
9. S. J. Boyes, P. J. Soh, Y. Huang, G. A. E. Vandenbosch, and N. Khiabani, "On-body performance of dual-band textile antennas," *IET microwaves, antennas PROPAG.*, vol. 6, no. 15, pp. 1696–1703, 2012, DOI: 10.1049/iet-map.2012.0469.
10. G.-P. Gao, C. Yang, B. Hu, R.-F. Zhang, and S.-F. Wang, "A wearable PIFA with an all-textile metasurface for 5 GHZ WBAN applications," *IEEE antennas WIREL. Propag. Lett.*, vol. 18, no. 2, pp. 288–292, 2019, DOI: 10.1109/lawp.2018.2889117.
11. l. K. & m. T. Husnu Yalduz, Burak koç, "an ultra-wideband low-SAR flexible metasurface-enabled antenna for WBAN applications," *Appl. Phys. A*, vol. 125, no. 9, p. 609, 2019, DOI: 10.1007/s00339-019-2902-4.
12. A. Y. I. Ashyap, Z. Zainal Abidin, S. H. Dahlan, H. A. Majid, and G. Saleh, "metamaterial inspired fabric antenna for wearable applications," *int. J. Rf MICROW. Comput. Eng.*, vol. 29, no. 3, pp. 1–10, 2019, DOI: 10.1002/mmce.21640.
13. a. Abdu, h. X. Zheng, h. A. Jabire, and m. Wang, "CPW-fed flexible monopole antenna with h and two concentric c slots on a textile substrate, backed by EBG for WBAN," *int. J. Rf MICROW. Comput. Eng.*, vol. 28, no. 7, pp. 1–7, 2018, DOI: 10.1002/mmce.21505.
14. r. A. Valenzuela, "antennas and propagation for wireless communications," *IEEE VEH. Technol. Conf.*, vol. 1, pp. 1–5, 1996, DOI: 10.1109/vetec.1996.503396.
15. H. Sugiyama and hi. Iwasaki, "Wearable finger ring dual band antenna made of fabric cloth for ban use," in *2013 7th EUROPEAN conference on antennas and propagation (EUCAP)*, 2013, pp. 3556–3559.
16. h. Goto and h. Iwasaki, "A low-profile wideband monopole antenna with a double finger ring a ban," in *2011 IEEE Aps topical conference on antennas and propagation in wireless communications*, 2011, pp. 409–412. Doi: 10.1109/apwc.2011.6046770.
17. a. Cihangir *et al.*, "Investigation of the effect of metallic frames on 4g eyewear antennas," *2014 LOUGHBRGH. Antennas PROPAG. Conf. LAPC 2014*, pp. 60–63, 2014, DOI: 10.1109/lapc.2014.6996320.
18. s.-w. Su and y.-t. Hsieh, "Integrated metal-frame antenna for smart-watch wearable device," *IEEE Trans. Antennas PROPAG.*, vol. 63, no. 7, pp. 3301–3305, 2015, DOI: 10.1109/tap.2015.2428736.
19. w. Hong, s. Lim, s. Ko, and y. G. Kim, "Optically invisible antenna integrated within an OLED touch display panel for IOT applications," *IEEE Trans. Antennas PROPAG.*, vol. 65, no. 7, pp. 3750–3755, 2017, DOI: 10.1109/tap.2017.2705127.
20. A. Y. I. Ashyap, z. Z. Abidin, s. H. Dahlan, h. A. Majid, and F. C. Seman, "A compact wearable antenna using EBG for smart-watch applications," in *2018 ASIA-pacific Microwave Conference (APMC)*, 2018, pp. 1477–1479. Doi: 10.23919/apmc.2018.8617196.

21. h.-s. Huang, h.-l. Su, and s.-l. Chen, "Multiband antennas for GPS/gsm1800/BLUTOOTH/wi-fi smart watch applications," in *2017 IEEE International Conference on Computational Electromagnetics (ICCEM)*, 2017, pp. 352–354. Doi: 10.1109/compem.2017.7912745.

22. C.-M. Cheng, W.-S. Chen, g.-q. Lin, and h.-m. Chen, "Four antennas on smartwatch for GPS/UMTS/ WLAN MIMO application," in *2017 IEEE International Conference on Computational Electromagnetics (ICCEM)*, 2017, pp. 346–348. Doi: 10.1109/compem.2017.7912744.

23. S. Hassan and S. H. Shehab, "Evaluation of an ultra-wideband (UWB) textile antenna in the vicinity of human body model for WBAN applications," in *2015 IEEE International WIE Conference on Electrical and Computer Engineering (WIECON-ECE)*, 2015, pp. 195–198. Doi: 10.1109/wiecon-ece.2015.7443895.

24. M. S. Shakhirul, M. Jusoh, A. H. Ismail, M. I. Jais, M. R. Kamarudin, and M. N. Osman, "Analysis of circular polarization textile antenna in bending condition," *i4ct 2015 - 2015 2nd int. Conf. Comput. Commun. Control technol. Art proceeding*, no. I4ct, pp. 360–363, 2015, DOI: 10.1109/i4ct.2015.7219598.

25. M. E. Lajevardi and M. Kamyab, "Ultraminiaturized metamaterial-inspired SIW textile antenna for off-body applications," *IEEE Antennas WIREL. Propag. Lett.*, vol. 16, pp. 3155–3158, 2017, DOI: 10.1109/lawp.2017.2766201.

26. W. A. M. Al Ashwal and k. N. Ramli, "Compact UWB wearable antenna with improved bandwidth and low SAR," *RFM 2013 - 2013 IEEE int. Rf MICROW. Conf. Proc.*, pp. 90–94, 2013, DOI: 10.1109/rfm.2013.6757225.

27. y. Hong, j. Tak, and j. Choi, "an all-textile Siw cavity-backed circular ring-slot antenna for WBAN applications," *IEEE antennas WIREL. Propag. Lett.*, vol. 15, no. C, pp. 1995–1999, 2016, DOI: 10.1109/lawp.2016.2549578.

28. g. Srivastava, a. Mohan, and A. Chakrabarty, "Compact reconfigurable UWB slot antenna for cognitive radio applications," *IEEE Antennas WIREL. Propag. Lett.*, vol. 16, pp. 1139–1142, 2017, DOI: 10.1109/lawp.2016.2624736.

29. Hevin A. Muhammad , Yadgar I. Abdulkarim, Peshwaz Abdulkareem Abdoul , Jian Dong ,"Textile and metasurface integrated wide-band wearable antenna for wireless body area network applications, " . 1434–8411, 2023, DOI: 10.1016.

30. Adel Y. I. Ashyap , Zuhairiah Zainal Abidin, Samsul Haimi Dahlan , Huda A. Majid, Muhammad Ramlee Kamarudin , Akram Alomainy, Raed A. Abd-Alhameed , Jamal Sulieman Kosha, and James M. Noras," Highly Efficient Wearable CPW Antenna Enabled by EBG-FSS Structure for Medical Body Area Network Applications,". *2018.*

31. Abbasi, M. A. B., Nikolaou, S. S., Antoniades, M. A., Nikolić Stevanović, M., & Vryonides, P. (2017). Compact EBG-Backed Planar Monopole for BAN Wearable Applications .IEEE Transactions on Antennas and Propagation, 65(2), 453-463.[7765040]. https://doi.org/10.1109/TAP.2016.2635588

32. Ameni Mersani, Osman Lotfi, Jean-Marc Ribero," Design of a textile antenna with artificial magnetic conductor for wearable applications, " .1338–1343, 2018, DOI: 10.1002.

33. C. Gabriel, "Compilation of the dielectric properties of body tissues at RF and microwave frequencies," 1996.

34. Rahman, H. M. Arifur, and Mohammad monirujjaman khan "Design and analysis of a compact band notch UWB antenna for body area network." Journal of electromagnetic analysis and applications 10(09):157. 2018.